DALTON
FULL PAPER

1,4-Dioxobenzene compounds of aluminium

Laura H. van Poppel,[a] Simon G. Bott[b] and Andrew R. Barron*[a]

[a] *Department of Chemistry and Center for Nanoscale Science and Technology, Rice University, Houston, Texas 77005, USA. E-mail: arb@rice.edu*
[b] *Department of Chemistry, University of Houston, Houston, Texas 77204, USA*

Received 25th April 2002, Accepted 28th June 2002
First published as an Advance Article on the web 6th August 2002

The aluminium aryloxide polymer, $[\{(^tBu)_2Al\}_2(\mu\text{-}OC_6H_4O)]_n$ (**1**) is synthesized by the addition of $Al(^tBu)_3$ to hydroquinone in a non-coordinating solvent, and reacts with Lewis bases, *via* both a solution and a solid/vapor reaction, to yield $[(^tBu)_2Al(L)]_2(\mu\text{-}OC_6H_4O)$ [L = py (**2**), 3,5-Me_2py (**3**) and THF (**4**)] *via* cleavage of the Al_2O_2 dimeric core. Thermolysis of **2**–**4** results in decomposition without clean formation of compound **1**. However, if compound **2** is formed by the exposure of **1** to pyridine vapors, subsequent thermolysis allows for the clean solid state interconversion of compounds **1** and **2**. The room temperature solid state reaction of $[\{(^tBu)_2Al\}_2(\mu\text{-}OC_6H_4O)]_n$ (**1**) with pyrazine (pz), 4,4′-bipyridine (4,4′-bipy) or 1,4-benzoquinone (1,4-bz) results in a rapid color change and the formation of $[\{(^tBu)_2Al\}_2(\mu\text{-}OC_6H_4O)(\mu\text{-}L)]_n$, where L = pz (**5**), 4,4′-bipy (**6**) and 1,4-bz (**7**).

Introduction

We have previously reported[1] that the gallium aryloxide polymer, $[\{(^tBu)_2Ga\}_2(\mu\text{-}OC_6H_4O)]_n$, synthesized by the addition of $Ga(^tBu)_3$ with hydroquinone in a non-coordinating solvent, reacts with pyridines, *via* both a solution and a solid/vapor reaction, to yield $[(^tBu)_2Ga(L)]_2(\mu\text{-}OC_6H_4O)$. The solid state thermolysis of $[(^tBu)_2Ga(L)]_2(\mu\text{-}OC_6H_4O)$ results in loss of the Lewis base and formation of the gallium aryloxide polymer; addition of the vapor of the appropriate ligand results in the solid state reformation of $[(^tBu)_2Ga(L)]_2(\mu\text{-}OC_6H_4O)$.

Given that aluminium alkoxides and aryloxides are known to undergo similar cleavage reactions with a wider range of Lewis bases as compared to their gallium homologs,[2] we have investigated the synthesis and reactivity of the aluminium aryloxide polymer, $[\{(^tBu)_2Al\}_2(\mu\text{-}OC_6H_4O)]_n$. In this regard, we report the synthesis of $[\{(^tBu)_2Al\}_2(\mu\text{-}OC_6H_4O)]_n$ and its interaction with pyridines, THF and a range of solid Lewis bases.

Results and discussion

The aluminium aryloxide polymer, $[\{(^tBu)_2Al\}_2(\mu\text{-}OC_6H_4O)]_n$ (**1**), may be synthesized by the addition of $Al(^tBu)_3$ to a suspension of hydroquinone in hexane at −78 °C (see Experimental). ^{13}C CPMAS NMR shows only a single set of resonances for the aryl *C*H groups and *tert*-butyl groups, suggesting that compound **1** is highly symmetrical (Fig. 1). The chemical shifts for the *tert*-butyl groups and the O–*C* carbons are essentially identical to the equivalent peaks found for the aluminium aryloxide dimer, $[(^tBu)_2Al(\mu\text{-}OPh)]_2$.[3]

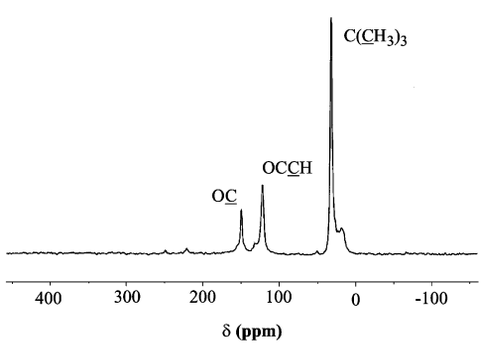

Fig. 1 ^{13}C CPMAS NMR spectrum of the aluminium aryloxide polymer, $[\{(^tBu)_2Al\}_2(\mu\text{-}OC_6H_4O)]_n$ (**1**).

^{27}Al MAS NMR was used to investigate the aluminium coordination environment in compound **1** and shows a single broad resonance (δ = 6 ppm, $W_{1/2}$ = 4030 Hz), (Fig. 2). This

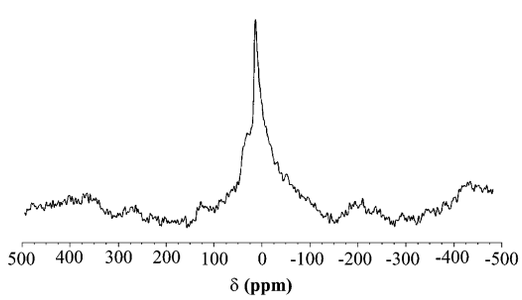

Fig. 2 ^{27}Al MAS NMR spectrum for $[\{(^tBu)_2Al\}_2(\mu\text{-}OC_6H_4O)]_n$ (**1**).

chemical shift is ordinarily associated with an octahedral aluminium coordination environment.[4] We have previously shown, however, that there are misconceptions about the relationship between chemical shift and coordination number.[5] For example, chemical shifts for three-coordinate aluminium compounds range between 276 and 3 ppm, while four-coordinate compounds have also been observed to cover a wide range, δ 140–47 ppm. Thus, chemical shift alone is not sufficient to characterize the coordination environment in compound **1**. If we compare the ^{27}Al NMR shift for compound **1** and $[(^tBu)_2Al(\mu\text{-}OPh)]_2$ (δ = 8 ppm, $W_{1/2}$ = 2550 Hz), for which the structure in solution and the solid state is known, it appears that the coordination around aluminium in compound **1** is analogous to that in $[(^tBu)_2Al(\mu\text{-}OPh)]_2$.[3] Interestingly, dialkylaluminium alkoxides, $[R_2Al(\mu\text{-}OR')]_2$ where $R' = C_nH_{2n+1}$, are known to exhibit ^{27}Al NMR shifts in the range of δ = 136–151 ppm.[6] The aluminium centers in compound **1** and $[(^tBu)_2Al(\mu\text{-}OPh)]_2$ are clearly in a very shielded (and asymmetric) environment. The shielded environment is presumably due to the phenyl rings since the upfield shifts are only observed for bridging aryloxides.

The NMR peak widths observed in ^{27}Al NMR spectroscopy provide information as to the symmetry about the aluminium

DOI: 10.1039/b204281a

nucleus in the compound under investigation. Narrow peaks are associated with high symmetry environments, *e.g.*, $[Al(OH)_4]^-$ and $[Al(H_2O)_6]^+$. In contrast, the line widths observed for compound **1** ($W_{1/2}$ = 4030 Hz) and $[(^tBu)_2Al(\mu\text{-}OPh)]_2$ ($W_{1/2}$ = 2550 Hz) are both typical of a highly asymmetric coordination environment about aluminium. The greater peak width observed for compound **1** is most probably due to the presence of slightly different AlO_2C_2 coordination environments, as compared to the single crystallographically unique environment observed for $[(^tBu)_2Al(\mu\text{-}OPh)]_2$.[3]

On the basis of the similarity in the chemical shifts and line widths, we propose that the aluminium aryloxide polymer has an Al_2O_2 dimeric core and structure typically observed for aluminium alkoxides.[6] It should be noted that the orientations of the phenoxide rings in $[(^tBu)_2Al(\mu\text{-}OPh)]_2$ are nearly perpendicular to the Al_2O_2 core and we propose a similar orientation is likely for compound **1**.

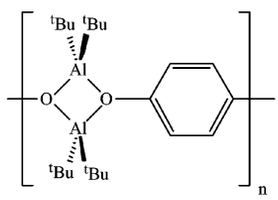

(**1**)

Compound **1** is insoluble in non-coordinating solvents, however, coordinating solvents, such as THF and pyridines allow for the dissolution of **1**. Dissolution of **1** in pyridine, 3,5-dimethylpyridine or THF results in cleavage of the Al_2O_2 dimeric core and results in the formation of the di-aluminium compounds, $[(^tBu)_2Al(L)]_2(\mu\text{-}OC_6H_4O)$, L = py (**2**), 3,5-$Me_2$py (**3**), and THF (**4**), respectively. Compound **1** is rapidly (minutes) converted to compounds **2** and **3** by dissolution in the appropriate Lewis base; the formation of compound **4** takes 2 days. This difference is comparable to previous observations of the cleavage of dimeric alkoxides and aryloxides.[2,7] Although compound **1** is converted to **2** by dissolution in pyridine (or reaction with pyridine in hydrocarbon solution), the reverse reaction is not as clean as the gallium analog, precluding the solid state transformation available to the gallium system. Compounds **2**–**4** are also prepared directly from the addition of two equivalents of $Al(^tBu)_3$ to a solution of hydroquinone (HOC_6H_4OH) in the appropriate Lewis base as a solvent. Similar reactions have been previously reported for the dimethylaluminium homologs.[8]

Compounds **2**–**4** are moisture sensitive, but only slightly oxygen sensitive. Each compound is soluble in its respective Lewis base, and also sparingly soluble in C_6H_6 and $CHCl_3$. Compounds **2** and **3** are yellow in color, while compound **4** is colorless. The UV/visible spectrum of compound **2** shows two absorptions at 303 and 329 nm, which are similar to those observed for its gallium analog.[1] The absorptions may be assigned to a ligand-to ligand charge transfer from a Al–C_σ to the low lying π^* orbital of the pyridine.[9]

The solid state structures of compounds **2**–**4** have been determined by X-ray crystallography and are shown in Fig. 3–5, respectively; selected bond lengths and angles are given in Table 1. The centrosymmetric molecular structures consist of a 1,4-dioxybenzene ligand bridging two $Al(^tBu)_2(L)$ moieties. The bond lengths around aluminium are within the ranges expected for such compounds.[2] Although the two $Al(^tBu)_2(L)$ units in each molecule are in an *anti* conformation, the 1,4-dioxybenzene ligand is not coplanar with the aluminium centers. The aluminium atoms are positioned on either side of the plane of the central 1,4-dioxybenzene ligand.

The geometry about aluminium is essentially unchanged between the pyridine, 3,5-Me_2py, or THF adducts. This invariance suggests that the steric bulk of THF and pyridine are comparable, since we have previously shown that the geometry about simple Lewis acid–base complexes is dependent on the steric bulk of the substituents.[10] In contrast, the Al–O–C bond angle varies significantly, from 139.4(2)° and 138.3(2)° for

Table 1 Selected bond lengths (Å) and angles (°) for $[(^tBu)_2Al(L)]_2(\mu\text{-}OC_6H_4O)$

L	py (**2**)	3,5-Me_2py (**3**)	THF (**4**)
Al–O	1.736(3)	1.727(2)	1.719(2)
Al–L	2.008(3)	1.997(3)	1.903(2)
Al–C	1.989(4)	1.965(5)	1.978(4)
	1.980(4)	2.006(5)	1.985(4)
O–Al–L	99.1(1)	96.6(1)	96.9(1)
O–Al–C	113.5(2)	111.8(2)	112.9(2)
	109.2(2)	109.8(2)	111.2(2)
L–Al–C	106.3(2)	108.4(2)	107.0(2)
	104.1(1)	103.1(2)	105.8(2)
C–Al–C	121.6(2)	123.4(3)	120.0(2)
Al–O–C	139.4(2)	138.3(2)	149.4(2)

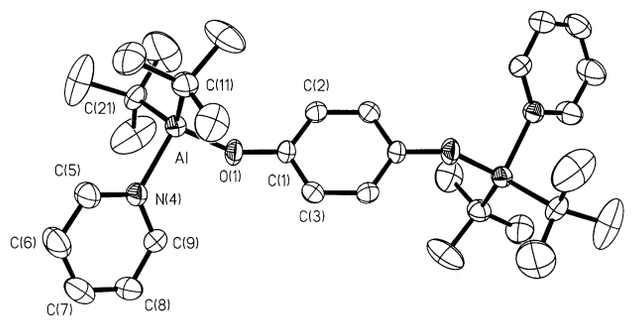

Fig. 3 Molecular structure of $[(^tBu)_2Al(py)]_2(\mu\text{-}OC_6H_4O)$ (**2**). Thermal ellipsoids shown at the 30% level, and hydrogen atoms are omitted for clarity.

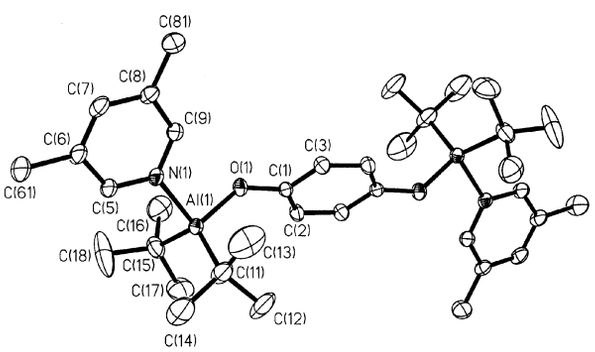

Fig. 4 Molecular structure of $[(^tBu)_2Al(3,5\text{-}Me_2py)]_2(\mu\text{-}OC_6H_4O)$ (**3**). Thermal ellipsoids shown at the 30% level, and hydrogen atoms are omitted for clarity.

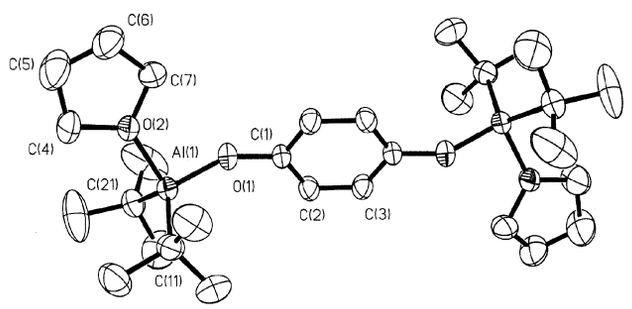

Fig. 5 Molecular structure of $[(^tBu)_2Al(THF)]_2(\mu\text{-}OC_6H_4O)$ (**4**). Thermal ellipsoids shown at the 30% level, and hydrogen atoms are omitted for clarity.

$$2[(^{t}Bu)_2Al(THF)]_2(\mu\text{-}OC_6H_4O) \overset{K_{eq}}{\rightleftharpoons} [\{(^{t}Bu)_2Al\}_2(\mu\text{-}OC_6H_4O)]_2 + 2THF \quad (1)$$

compound **2** and **3**, respectively, to 149.4(2)° for compound **4**. This difference is possibly due to the difference in donor ability for each Lewis base, *i.e.*, pyridine is a stronger donor than THF, resulting in a decrease in donation from the aryloxide oxygen. However, the Al–O bond distance in compound **4** is slightly, but not significantly, shorter than that in compounds **2** and **3** (see Table 1). An alternative rationale is that the Al ··· Al distance (and therefore the Al–O–C angle) is a function of crystal packing which is controlled by the identity of the Lewis base.

Unlike the gallium analogs,[1] the solution ^{1}H and ^{13}C NMR spectra of compounds **2** and **3** show only one set of resonances, which is consistent with $[(^{t}Bu)_2Al(L)]_2(\mu\text{-}OC_6H_4O)$. In contrast, the solution ^{1}H and ^{13}C NMR spectra of compound **4** show two sets of resonances, the first can be assigned to $[(^{t}Bu)_2Al(THF)]_2(\mu\text{-}OC_6H_4O)$, while the second is consistent with dissociation of one molecule of THF per equivalent of compound **4**. Variable temperature NMR indicates that an equilibrium is present [eqn. (1)], although the presence of two sets of resonances indicates that the reaction is slow on the NMR time scale (10^{-5} s). Compound **4** could not be isolated in a pure state, but similar results have been published by Gabbaï and co-workers, who reported the dimethylaluminium analogue (**I**).[8]

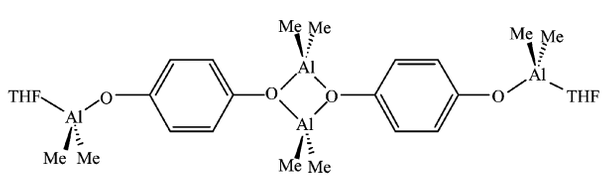

The aluminium aryloxide polymer, $[\{(^{t}Bu)_2Al\}_2(\mu\text{-}OC_6H_4O)]_n$ (**1**), reacts with vapors of pyridine, 3,5-Me_2py and THF to form compounds **2**–**4**. Unlike their gallium analogs the thermogravimetric/differential thermal analysis (TG/DTA) of compounds **2** and **3** do not show a well-defined step associated with the loss of the Lewis base before decomposition to Al_2O_3. In contrast, compound **4** shows an endotherm at 170 °C (melting point), and then decomposes to Al_2O_3. If compound **1** is reacted with pyridine vapor and the TG/DTA of the subsequent product (*i.e.*, **2**) shows a distinct loss of two molar equivalents of pyridine (31%, calc. 29%), see Fig. 6. Based on what we know about the reactivity of the gallium analogs, this observation suggests that the molecular packing of compound **2**, when crystallized from pyridine, is different from that formed from the vapor phase reaction of compound **1** with pyridine.

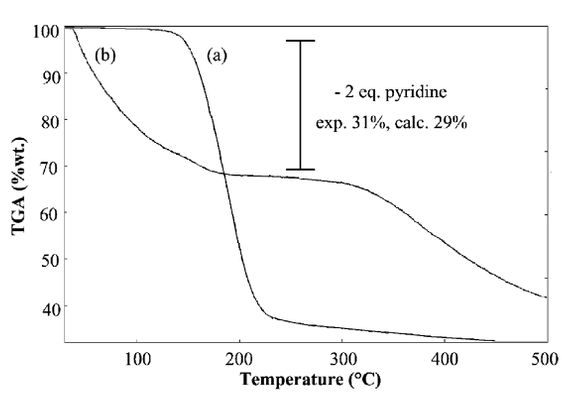

Fig. 6 TG/DTA of (a) $[(^{t}Bu)_2Al(py)]_2(\mu\text{-}OC_6H_4O)$ (**2**) crystallized from pyridine solution, and (b) the product from the reaction of $[\{(^{t}Bu)_2Al\}_2(\mu\text{-}OC_6H_4O)]_n$ (**1**) with pyridine vapor.

Table 2 Selected ^{13}C NMR chemical shifts

Compound	δ/ppm		
	O*C*	C(CH_3)$_3$	N*C*
$[\{(^{t}Bu)_2Al\}_2(\mu\text{-}OC_6H_4O)]_n$ (**1**)	149.3	31.8	
$[\{(^{t}Bu)_2Al\}_2(\mu\text{-}OC_6H_4O)(\mu\text{-pz})]_n$ (**5**)	149.8	31.3	144.5
$[(^{i}Pr)_3Al]_2(\mu\text{-pz})$ [a]			144.0
pz			146.1
$[\{(^{t}Bu)_2Al\}_2(\mu\text{-}OC_6H_4O)\text{-}(\mu\text{-4,4′-bipy})]_n$ (**6**)	151.8	31.6	147.8
$[(^{i}Pr)_3Al]_2(\mu\text{-4,4′-bipy})$ [a]			148.4
4,4′-bipy			151.6

[a] Ref. 11.

The room temperature solid state reaction of $[\{(^{t}Bu)_2Al\}_2(\mu\text{-}OC_6H_4O)]_n$ (**1**) with 4,4′-bipyridine (4,4′-bipy), pyrazine (pz) or 1,4-benzoquinone (1,4-bz) results in a rapid color change from colorless to orange, yellow and purple, respectively (*e.g.*, Fig. 7). When these products are washed with ether or CH_2Cl_2 to get rid of any excess ligand, the color still remains (Fig. 8).

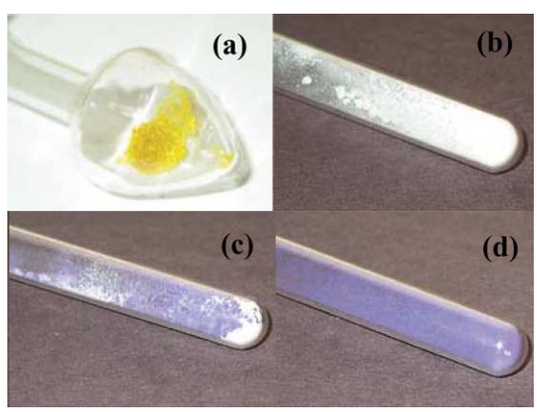

Fig. 7 Photographs showing the color changes observed for the solid state reaction of (a) 1,4-benzoquinone with (b) $[\{(^{t}Bu)_2Al\}_2(\mu\text{-}OC_6H_4O)]_n$ (**1**) at (c) one minute and (d) five minutes after mixing.

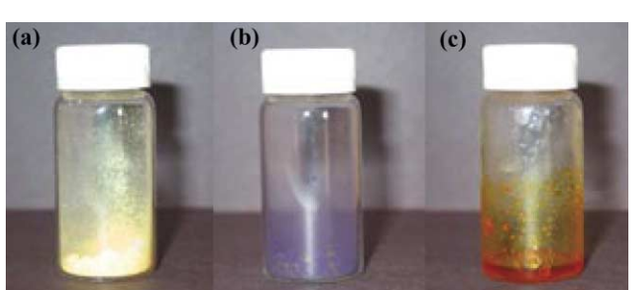

Fig. 8 Pictures of (a) $[\{(^{t}Bu)_2Al\}_2(\mu\text{-}OC_6H_4O)(\mu\text{-pz})]_n$ (**5**) and (b) $[\{(^{t}Bu)_2Al\}_2(\mu\text{-}OC_6H_4O)(\mu\text{-1,4-bz})]_n$ (**7**) after solid state mixing at room temperature, and (c) $[\{(^{t}Bu)_2Al\}_2(\mu\text{-}OC_6H_4O)(\mu\text{-4,4′-bipy})]_n$ (**6**) after heating to 110 °C for 30 seconds.

The MS of each product shows the presence of the appropriate Lewis base, however, elemental analysis is consistent with the presence of unreacted $[\{(^{t}Bu)_2Al\}_2(\mu\text{-}OC_6H_4O)]_n$ (**1**). However, the ^{13}C CPMAS NMR spectra suggests the formation of $[\{(^{t}Bu)_2Al\}_2(\mu\text{-}OC_6H_4O)(\mu\text{-L})]_n$, where L = pz (**5**), 4,4′-bipy (**6**) and 1,4-bz (**7**). The ^{13}C CPMAS NMR signals of the α-*C* on the pz (**5**) and 4,4′-bipy (**6**) exhibit an upfield shift when compared to the α-*C* of the uncomplexed ligand. These results are in agreement with previously reported $Al(^{i}Pr)_3$ interactions with these ligands (Table 2).[11]

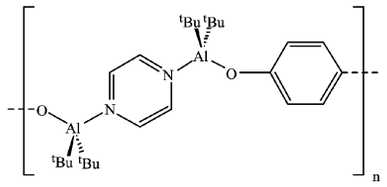

(5)

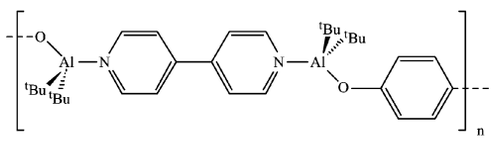

(6)

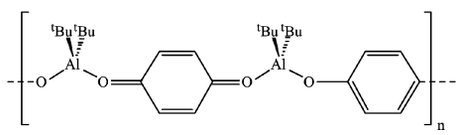

(7)

Compounds **5**–**7** are insoluble in most organic solvents and dissociation of the ligand occurs in coordinating solvents; therefore, solution ^{1}H and ^{13}C NMR could not be obtained. But, in the case of compounds **5** and **6**, the Al : L ratio may be confirmed as 2 : 1 from the relative integration of *tert*-butyl groups and the ligand resonances in the ^{1}H NMR in d_5-py solution, *i.e.*, eqn. (2).

$$[\{(^{t}Bu)_2Al\}_2(\mu\text{-}OC_6H_4O)(\mu\text{-}L)] + py(xs) \longrightarrow [(^{t}Bu)_2Al(py)]_2(\mu\text{-}OC_6H_4O) + L \quad (2)$$

Given the rapid reaction between compound **1** and these bifunctional Lewis bases it is unlikely that their formation is purely a solid state diffusion reaction. Instead, we propose that the formation of compounds **5**–**7** occurs as a consequence of each Lewis base having a sufficient vapor pressure such that a vapor/solid reaction occurs.

The ^{27}Al MAS NMR spectrum for compound **7** exhibits a single peak (δ = 22 ppm, Fig. 9) which has been previously

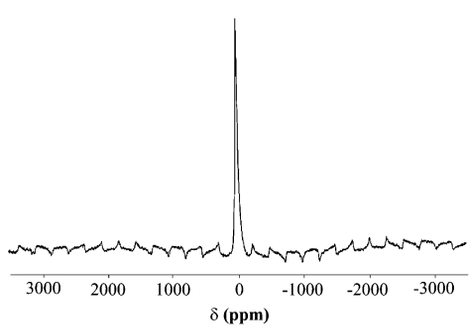

Fig. 9 ^{27}Al MAS NMR spectrum for $[\{(^{t}Bu)_2Al\}_2(\mu\text{-}OC_6H_4O)(\mu\text{-}1,4\text{-bz})]_n$ (**7**).

assigned to either a four- or five-coordinate aluminium,[12] although if it is a four-coordinate environment it would be considered a shielded environment. However, given the chemical shift observed for the AlO_2C_2 coordination environment in compound **1** and $[(^{t}Bu)_2Al(\mu\text{-}OPh)]_2$, the shift for compound **7** would not be unexpected.

The ^{27}Al MAS NMR spectra for compounds **5** and **6** exhibit complex spectra with a centerband around 6 ppm. As may be seen from Fig. 10a, the spectrum of compound **6** consists of three peaks and two shoulders which span 30 kHz. Spectra were taken at varying spinning speeds (20, 30 and 33 kHz) in order to

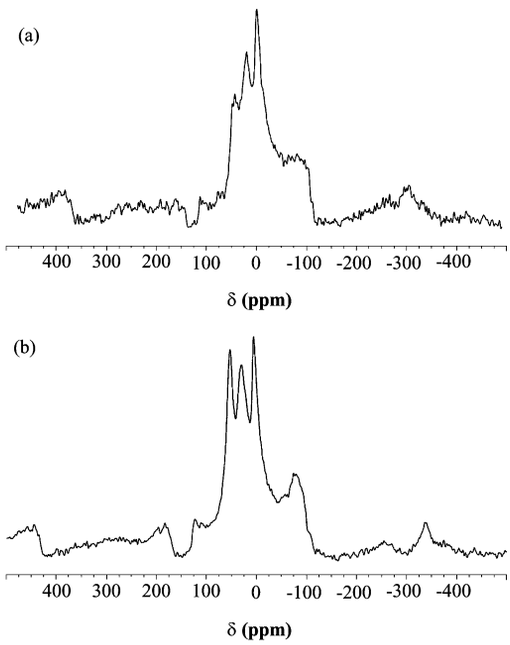

Fig. 10 ^{27}Al MAS NMR spectra for (a) $[\{(^{t}Bu)_2Al\}_2(\mu\text{-}OC_6H_4O)(\mu\text{-}4,4'\text{-bipy})]_n$ (**6**) and (b) $[(^{t}Bu)_2Al(OPh)]_2(\mu\text{-}4,4'\text{-bipy})$ (**II**).

determine the difference between center- and side-bands. The three center peaks remained the same, but the shoulders did not become apparent until a higher spinning speed was employed. The overall line shape varied with each spinning speed, so we cannot say with any certainty that if the sample was spun infinitely fast that this would be the final spectra. Furthermore, in order to decipher these spectra, we would need to compare them to those taken at higher field strengths, especially if the quadrupole coupling constant is large.[13] The higher magnetic field would reduce any broadening of the signal for the central transition. The ^{27}Al MAS NMR spectrum for compound **6** is very similar to that observed (Fig. 10b) for the crystallographically characterized $[(^{t}Bu)_2Al(OPh)]_2(\mu\text{-}4,4'\text{-bipy})$ (**II**) suggesting that the solid state coordination environments are the same.[14]

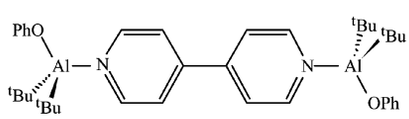

(II)

Experimental

Mass spectra were obtained on a Finnigan MAT 95 mass spectrometer operating with an electron beam energy of 70 eV for EI mass spectra. IR spectra (4000–400 cm^{-1}) were obtained using an Nicolet 760 FT-IR infrared spectrometer. Solution ^{1}H and ^{13}C NMR spectra were obtained on Bruker Avance 200, 400, and 500 MHz spectrometers. Chemical shifts are reported relative to internal solvent resonances (^{1}H and ^{13}C), and external $[Al(H_2O)_6]^{3+}$ (^{27}Al). Solid state ^{13}C CPMAS (cross polarization, magic angle spinning) NMR spectra were measured on a Bruker Avance 200 spectrometer at 50.3 MHz. Samples were measured in a 7 mm or 4 mm ZrO_2 rotor. Typical measurement conditions were as follows: spinning frequency, 5 kHz; pulse repetition time, 5 s; spectral width, 31 kHz; number of points, 2k; number of scans, 10k; contact time 2 ms. Chemical shifts in ^{13}C CPMAS spectra were referred to the carbonyl band of glycine (with a signal at 176.0 ppm) by sample replacement. ^{27}Al MAS NMR spectra were obtained on a Bruker Avance 500 MHz spectrometer. All rotors were loaded in argon filled gloveboxes and transported to the NMR in

capped vials. The 2.5 mm ZrO_2 rotors and tight fitting Kel–F caps were spun with air to 20–35 kHz. Chemical shifts were set *via* 1 M $Al(NO_3)_3$ (aq) to 0 ppm. Pulse power was set with 1 M $Al(NO_3)_3$ (aq) to give a 0.95 μs 90° pulse. A 0.5 μs pulse was used with an accumulation of 2400–7000 scans. Microanalyses were performed by Oneida Research Services, Inc., Whitesboro, NY. Thermogravametric analyses were performed on a Seiko I TG/DTA 200. The synthesis of $Al(^tBu)_3$ was performed according to a modification of the literature method.[15] HOC_6H_4OH, pyridine, 3,5-dimethylpyridine, and THF were obtained from Aldrich and (except for HOC_6H_4OH) were distilled over N_2 and stored over Na metal prior to use. All manipulations were performed under an inert atmosphere of argon or nitrogen. Solvents were distilled and degassed prior to use.

Synthesis

$[\{(^tBu)_2Al\}_2(\mu\text{-}OC_6H_4O)]_n$ (1). To a cooled (−78 °C) suspension of hydroquinone (0.606 g, 5.5 mmol) in hexane (100 mL) was added $Al(^tBu)_3$ (3.00 mL, 12.1 mmol). The solution was allowed to warm to room temperature and stir for 18 h producing a white powder. Yield: 1.7 g, 79%. MS (EI, %): *m*/*z*, 1000 ($3M^+ - 3^tBu$, 20), 667 ($2M^+ - 2^tBu$, 100), 335 ($M^+ - {}^tBu$, 20). IR (cm^{-1}): 1378 (s), 1295 (w), 1195 (s), 1101 (w), 1000 (w) 930 (w), 930 (w), 841 (m), 800 (s), 724 (w), 612 (m). ^1H NMR (d_5-pyridine): δ 7.07 (4H, s, C_6H_4), 1.19 [36H, s, $C(CH_3)_3$]. ^{13}C NMR (d_5-pyridine): δ 153.2 (O*C*), 120.6 (OC*C*H), 31.4 [C(CH_3)$_3$]. ^{13}C CPMAS NMR: δ 149.3 (O*C*), 121.4 (OC*C*H), 31.8 [C(CH_3)$_3$]. ^{27}Al MAS NMR: δ 6 ($W_{1/2}$ = 4030 Hz).

$[(^tBu)_2Al\}(\mu\text{-}OC_6H_5)]_2$. Prepared according to literature procedures.[3] ^{13}C CPMAS NMR: δ 153.4 (O*C*), 131.8 (*o*-*C*H), 125.9 (*m*-*C*H), 119.6 (*p*-*C*H), 32.6 [C(CH_3)$_3$]. ^{27}Al NMR: δ 8 ($W_{1/2}$ = 2550 Hz).

$[(^tBu)_2Al(py)]_2(\mu\text{-}OC_6H_4O)$ (2). To a cooled (−78 °C) suspension of hydroquinone (0.423 g, 3.80 mmol) in pyridine (30 mL) was added $Al(^tBu)_3$ (2.0 mL, 8.0 mmol). The solution was allowed to warm to room temperature and stir for 18 h. The clear, yellow solution was cooled to −30 °C overnight yielding crystals suitable for single crystal X-ray analysis. Yield: 2.6 g, 87%. Elemental analysis (calc. %): C, 68.67 (70.07); H, 8.74 (9.12); N, 5.09 (5.11). MS (CI, $Me_2C{=}CH_2$, %): *m*/*z* 139 [$Al(^tBu)_2$, 15], 111 (OC_6H_4O, 20), 80 (py, 30), 57 (^tBu, 100). IR (cm^{-1}): 1612 (m), 1375 (s), 1256 (s), 1210 (m), 1067 (m), 1041 (s), 999 (m), 877 (s), 832 (m), 812 (s), 754 (m), 700 (s), 666 (w), 650 (m). ^1H NMR ($CDCl_3$): δ 8.85 [4H, d, *J*(H–H) = 6 Hz, NC*H*], 8.1 [2H, t, *J*(H–H) = 7 Hz, *p*-C*H*], 7.69 [4H, t, *J*(H–H) = 6.5 Hz, *m*-C*H*], 6.66 (4H, s, C_6H_4), 0.91 [36H, s, $C(CH_3)_3$]. ^{13}C NMR ($CDCl_3$): δ 152.2 (O*C*), 147.9 (N*C*H), 141.2 (*p*-*C*H), 125.7 (*m*-*C*H), 119.7 (OC*C*H), 30.7 [C(CH_3)$_3$]. UV: λ = 303 nm (ε = 4300 L mol^{-1} cm^{-1}), λ = 329 nm (ε = 1200 L mol^{-1} cm^{-1}).

$[(^tBu)_2Al(3,5\text{-}Me_2py)]_2(\mu\text{-}OC_6H_4O)$ (3). $[\{(^tBu)_2Al\}_2(\mu\text{-}OC_6H_4O)]_n$ (0.15 g, 0.38 mmol) was dissolved in 3,5-lutidine (15 mL) and allowed to stir for 18 h. The clear yellow solution was cooled to −30 °C overnight yielding crystals suitable for single crystal X-ray analysis. Yield: 0.19 g, 82%. MS (EI, %): *m*/*z* 667 ($M^+ - 2^tBu - 2Me_2py$, 100), 107 (Me_2py, 98). IR (cm^{-1}): 1854 (w), 1608 (m), 1383 (s), 1265 (s), 1183 (m), 1152 (s), 1091 (m), 1040 (m), 1009 (m), 927 (m), 871 (s), 835 (s), 809 (s), 789 (s), 702 (s). ^1H NMR ($CDCl_3$): δ 8.60 (2H, s, NC*H*), 7.70 (4H, s, *p*-C*H*), 6.66 (4H, s, OCC*H*), 2.45 (12H, s, CH_3), 0.90 [36H, s, $C(CH_3)_3$]. ^{13}C NMR ($CDCl_3$): δ 152.3 (O*C*), 145.1 (N*C*H), 142.4 (*p*-*C*H), 135.3 (*m*-*C*H), 119.7 (OC*C*H), 30.8 [*C*(CH_3)$_3$], 23.4 [C(CH_3)$_3$], 18.8 (CH_3).

$[(^tBu)_2Al(THF)]_2(\mu\text{-}OC_6H_4O)$ (4). To a cooled (−78 °C) suspension of hydroquinone (0.606 g, 5.5 mmol) in THF (40 mL) was added $Al(^tBu)_3$ (3.0 mL, 12.1 mmol). The solution was allowed to warm to room temperature and stir for 18 h. The clear, colorless solution was cooled to −30 °C overnight yielding crystals suitable for single crystal X-ray analysis. Yield: 2.5 g, 86%. Mp: 165–170 °C. MS (EI, %): *m*/*z* 535 (M^+ + H, 5). IR (cm^{-1}): 1383 (s), 1255 (m) 1081 (m), 1004 (m), 906 (m), 799 (m). ^1H NMR ($CDCl_3$): δ 6.72 (4H, s, C_6H_4), 3.75 (8H, m, O*C*H_2), 1.86 (8H, m, CH_2), 1.01 [36H, s, C(CH_3)$_3$]. ^{13}C CPMAS NMR: δ 152.0 (O*C*), 120.0 (OC*C*H), 73.9 (O*C*H_2), 31.6 [C(*C*H_3)$_3$], 25.7 (*C*H_2). ^{27}Al MAS NMR: δ 5, 116, −136, ($W_{1/2}$ = 1850, 670, 2320 Hz).

$[\{(^tBu)_2Al\}_2(\mu\text{-}OC_6H_4O)(\mu\text{-}pz)]_n$ (5). A 100 mL round bottom flask was charged with $[\{(^tBu)_2Al\}_2(\mu\text{-}OC_6H_4O)]_n$ (0.5 g, 1.26 mmol) and pyrazine (0.21 g, 2.5 mmol). After 5 minutes the solid had changed color from white to yellow. The solid was dissolved in CH_2Cl_2 (30 mL) in order to wash the product of excess pyrazine. The solution was allowed to stir for 18 h. A bright yellow insoluble powder and a light yellow solution were produced. The yellow powder was collected and analyzed. Yield: 0.5 g, 88%. Elemental analysis (calc., %): C, 64.3 (66.3); H, 9.08 (9.36); N, 2.74 (5.96). MS (EI, %): *m*/*z* 333 ($M^+ - Bu$, 100), 80 (pz, 99). IR (cm^{-1}): 2928 (m), 2867 (w), 2837 (s), 1506 (s), 1467 (m), 1411 (w), 1359 (w), 1225 (w), 1195 (s), 1100 (w), 10005 (w), 849 (m), 806 (s). ^1H NMR (d_5-pyridine): δ 8.61 (1H, s, NC*H*), 7.19 (1H, s, NC*H*), 7.08 (4H, s, OC*H*), 1.19 [36H, s, C(CH_3)$_3$]. ^{13}C CPMAS NMR: δ 149.8 (O*C*), 120.6 (OC*C*H), 31.3 [C(*C*H_3)$_3$]. ^{27}Al MAS NMR: δ 25, 24 ($W_{1/2}$ = 7690 Hz).

$[\{(^tBu)_2Al\}_2(\mu\text{-}OC_6H_4O)(\mu\text{-}4,4'\text{-}bipy)]_n$ (6). Prepared in the same manner as compound **5** using $[\{(^tBu)_2Al\}_2(\mu\text{-}OC_6H_4O)]_n$ (0.5 g, 1.26 mmol) and 4,4′-bipyridyl (0.40 g, 2.5 mmol). After 5 minutes, the reactants changed color from white to orange. The reactants were suspended in Et_2O (30 mL) in order to wash the product of excess 4,4′-bipyridyl. The solution was stirred for 18 h. A bright orange insoluble powder, and a light orange solution were produced. The orange powder was collected and analyzed. Yield: 0.5 g, 71%. MS (EI, %): *m*/*z* 333 (M^+ − 4,4′-bipy − ^tBu, 60), 156 (4,4′-bipy, 100), 57 (^tBu, 90). IR (cm^{-1}): 2941 (w), 2929 (m), 2859 (w), 2820 (s), 1618 (m), 1506 (s), 1463 (m), 1411 (w), 1268 (m), 1216 (m), 1069 (w), 1000 (w), 879 (m), 832 (w), 810 (s). ^1H NMR (d_5-pyridine): δ 8.87 [2H, d of d, *J*(H–H) = 2.8, 6.1 Hz, NC*H*], 7.61 [2H, d of d, *J*(H–H) = 2.8, 6.1 Hz, *m*-C*H*], 7.07 (1H, s, OC*H*), 1.19 [9H, s, C(CH_3)$_3$]. ^{13}C CPMAS: δ 151.8 (O*C*), 147.8 (N*C*H), 144.2 (*m*-*C*H), 119.9 (OC*C*H), 31.6 [C(*C*H_3)$_3$]. ^{27}Al MAS NMR: δ 52, 29, 7 ($W_{1/2}$ = 9640 Hz).

$[\{(^tBu)_2Al\}_2(\mu\text{-}OC_6H_4O)(\mu\text{-}1,4\text{-}bz)]_n$ (7). Prepared in the same manner as compound **4** using $[\{(^tBu)_2Al\}_2(\mu\text{-}OC_6H_4O)]_n$ (0.5 g, 1.28 mmol) and 1,4-benzoquinone (0.277 g, 2.56 mmol). The color of the reactants changed immediately from white and yellow to light purple and became progressively darker purple for the next 5 minutes. This mixture was suspended in ether (30 mL) in order to wash the product of excess 1,4-benzoquinone. The solution was allowed to stir for 18 h, whereupon a deep purple insoluble powder was filtered from a light purple solution. Yield: 0.47 g, 74%. MS (EI, %): *m*/*z* 333 ($M^+ - {}^tBu$, 100), 110 [(OC_6H_4O), 98]. IR (cm^{-1}): 3334 (w), 3036 (w), 2958 (w), 2842 (w), 1601 (w), 1506 (s), 1195 (m), 1095 (w), 832 (s). ^{13}C CPMAS NMR: δ 149.4 (O*C*), 120.5 (OC*C*H), 31.7 [C(*C*H_3)$_3$]. ^{27}Al MAS NMR: δ 22 ($W_{1/2}$ = 4790 Hz).

Crystallographic studies

Data for compounds **2**–**4** were collected on a Bruker CCD SMART system, equipped with graphite monochromated Mo-Kα radiation (λ = 0.71073 Å) and corrected for Lorentz and polarization effects. Data collection and unit cell and space group determination were all carried out in the usual manner.[16] The structures were solved using the direct methods program

Table 3 Summary of X-ray diffraction data

Compound	$[(^tBu)_2Al(py)]_2$-(μ-OC_6H_4O) (**2**)	$[(^tBu)_2Al(3,5\text{-}Me_2py)]_2$ (μ-OC_6H_4O) (**3**)	$[(^tBu)_2Al(THF)]_2$-(μ-OC_6H_4O) (**4**)
Empirical formula	$C_{32}H_{50}Al_2N_2O_2$	$C_{36}H_{58}Al_2N_2O_2$	$C_{30}H_{56}Al_2O_4$
M_w	548.70	604.81	534.71
Crystal system	Monoclinic	Monoclinic	Monoclinic
Space group	$P2_1/c$	$P2_1/n$	$P2_1/n$
a/Å	8.621(2)	10.983(2)	8.455(2)
b/Å	12.516(3)	13.960(3)	12.306(3)
c/Å	16.124(3)	12.837(3)	16.489(3)
β/°	100.90(3)	96.85(3)	104.67(3)
V/Å^3	1708.5(6)	1954.1(7)	1659.7(6)
Z	2	2	2
D_{calc}/g cm^{-3}	1.067	1.028	1.070
μ_{calc}/mm^{-1}	2.11	0.104	0.117
No. collected reflections	4377	8798	4275
No. independent reflections	1990	2829	2107
No. observed reflections (weighting scheme)	1102 ($\|F_o\| > 4.0\sigma\|F_o\|$)	1584 ($\|F_o\| > 4.0\sigma\|F_o\|$)	1444 ($\|F_o\| > 4.0\sigma\|F_o\|$)
SHELXTL parameters	0.064, 0	0.1305, 0	0.1176, 0
R	0.0481	0.0626	0.0604
R_w	0.1166	0.1812	0.1712

XS[17] and difference Fourier maps and refined by using full matrix least squares methods. All non-hydrogen atoms were refined with anisotropic thermal parameters. Hydrogen atoms were introduced in calculated positions and allowed to ride on the attached carbon atoms [d(C–H) = 0.95 Å]. Refinement of positional and anisotropic thermal parameters led to convergence (see Table 3).

CCDC reference numbers 187090–187092.

See http://www.rsc.org/suppdata/dt/b2/b204281a/ for crystallographic data in CIF or other electronic format.

Acknowledgements

Financial support for this work is provided by the Robert A. Welch Foundation, including the Bruker CCD Smart System Diffractometer of the Texas Center for Crystallography at Rice University. The Bruker Avance 200 and 500 NMR spectrometers were purchased with funds from ONR Grant N00014-96-1-1146 and NSF Grant CHE-9708978, respectively.

References

1 L. H. van Poppel, S. G. Bott and A. R. Barron, *J. Am. Chem. Soc.*, submitted for publication.
2 S. J. Obrey, S. G. Bott and A. R. Barron, *Organometallics*, 2001, **20**, 5119; M. D. Healy, J. W. Ziller and A. R. Barron, *J. Am. Chem. Soc.*, 1990, **112**, 2949.
3 C. L. Aitken and A. R. Barron, *J. Chem. Crystallogr.*, 1996, **26**, 293.
4 See for example, D. A. Atwood, J. A. Jegier and D. Rutherford, *Inorg. Chem.*, 1996, **35**, 63.
5 A. R. Barron, *Polyhedron*, 1995, **14**, 3197.
6 J. H. Rogers, A. W. Apblett, W. M. Cleaver, A. N. Tyler and A. R. Barron, *J. Chem. Soc., Dalton Trans.*, 1992, 3179.
7 M. D. Healy, M. B. Power and A. R. Barron, *J. Coord. Chem.*, 1990, **21**, 363.
8 F. A. R. Kaul, M. Tschinkl and F. P. Gabbaï, *J. Organomet. Chem.*, 1997, **539**, 187.
9 J. Baumgarten, C. Bessenbacher, W. Kaim and T. Stahl, *J. Am. Chem. Soc.*, 1989, **111**, 2126.
10 J. A. Francis, C. N. McMahon, S. G. Bott and A. R. Barron, *Organometallics*, 1999, **21**, 4399.
11 S. Hasenzahl, W. Kaim and T. Stahl, *Inorg. Chim. Acta*, 1994, **225**, 23.
12 C. A. Fyfe, J. L. Bretherton and L. Y. Lam, *J. Am. Chem. Soc.*, 2001, **123**, 5285.
13 L. B. Alemany, S. Steuernagel, J.-P. Amoureux, R. L. Callender and A. R. Barron, *Solid State Nucl. Magn. Reson.*, 1999, **14**, 1.
14 L. H. van Poppel, D. Orgin, S. G. Bott and A. R. Barron, *Organometallics*, submitted for publication.
15 W. Uhl, *Z. Anorg. Allg. Chem.*, 1989, **570**, 37; H. Lehmkuhl, O. Olbrysch and H. Nehl, *Liebigs Ann. Chem.*, 1973, 708; H. Lehmkuhl and O. Olbrysch, *Liebigs Ann. Chem.*, 1973, 715.
16 M. R. Mason, J. M. Smith, S. G. Bott and A. R. Barron, *J. Am. Chem. Soc.*, 1993, **115**, 4971.
17 G. M. Sheldrick, SHELXTL, Bruker AXS, Inc., Madison, Wisconsin, 1997.